技術論文

A Study on Optimal Combinations of Winding and Cooling Methods for Downsizing Power Units in Motorcycles

Ryota Otaki　Teruyuki Tsuchiya　Yu Sakai　Takuya Yamauchi　Tsukasa Shimizu

当論文は、JSAE 20249007/SAE 2024-32-0007として、SETC2024（Small Powertrains and Energy Systems Technology Conference）にて発表されたものです。

要旨

市販されている電動バイクでは、出力の増加に伴い、冷却方式は空冷から水冷へ、巻線方式は集中巻から分布巻へと変化する傾向が見られる。この変化は8~10kW 付近で起こる。しかし、これらの冷却方式と巻線方式の組み合わせが最適であるかどうかを検証した研究は少ない。この傾向を検証するために、車両の要求出力と熱性能に応じてモータと冷却システムの合計容量と重量を比較できる検証モデルを構築した。構築したモデルを用いて、巻線方式（集中巻またはセグメントコンダクタ（SC）分布巻）と冷却方式（水冷または空冷）の組み合わせの比較検証を行った。本研究で設計したモータにおいて、車両の最大出力が35kW 以下（欧州 A2免許範囲）の場合、モータと冷却システムの合計体積は空冷集中巻モータが最も小さいことがわかった。しかし、15kW 以上では、冷却装置（ラジエータ、ホース、ポンプ、リザーバタンク、冷却水）を含む水冷式 SC モータの体積は、空冷集中巻モータの約110％であることが分かった。また、重量は約65％以下であった。本研究では、分布巻モータの一種として SC モータを検討したが、分布巻モータの特徴として、スロット数が多く、巻線とステータコアの接触面積が大きく、放熱性が高いことが挙げられる。これらの特性は巻線種類に関係なく共通である。したがって、上記の知見は、定格出力が約10kW の EV において、水冷分布巻モータの採用が増加しているという市場傾向とおおむね一致している。

Abstract

In commercially available electric motorcycles, there is a notable shift in the cooling method, moving from air cooling to water cooling, and in the winding method, moving from concentrated winding to distributed winding, as the output increases. This shift occurs around 8 to 10 kW. However, there is a paucity of empirical investigations examining these combinations to ascertain their optimality.

In order to verify this trend, a verification model has been constructed which allows for the comparison of the capacity and weight of the motor and cooling system according to the vehicle's required output and thermal performance. A comparison and verification of the combinations of winding methods (concentrated winding or segment conductor distribution winding) and cooling systems (water-cooled or air-cooled) was conducted using the model that had been constructed.

In the motor designed for this study, when the maximum output of the vehicle was 35 kW or less (European A2 license), the total volume of the motor and cooling system was found to be the smallest for the air-cooled concentrated winding motor. However, in the 15 kW and above range, it was found that the volume of the water-cooled Segment conductor (SC) winding motor, including the cooling system (radiator, hoses, pump, reservoir tank, cooling water), was approximately 110% of the air-cooled concentrated winding motor, and the weight was approximately 65% or less. In this study, we used a SC winding motor as a type of distributed winding motor for verification. The characteristics of distributed winding motors include a large number of slots that provide a large contact area with the winding and high heat dissipation. These characteristics are the same regardless of the type of winding. Therefore, these findings are generally consistent with the observed trend of an increasing adoption of water-cooled distributed-winding motors in commercially available electric vehicles (EVs) with a power rating of approximately 10 kW.

1 INTRODUCTION

In power units (PU) for motorcycles, it is important to achieve a compact and lightweight design. When downsizing the motor, temperature rise becomes a problem. Therefore, in order to design a compact and lightweight motor, it is necessary to design a proper cooling structure. In the previous study[1], various motor cooling methods, including water cooling and air cooling, were compared. Air cooling provides a simple cooling system, but there is concern that the cooling capacity may not be sufficient for high power motors. Water cooling requires components such as a radiator in addition to the motor, and the increase in volume and weight must be considered.

Figure 1 shows the combinations of winding and cooling methods for each output for EVs currently on the market. There is a switch between water cooling and air cooling at around 8 to 10 kW, and there is also a trend for the winding to switch from concentrated winding to distributed winding.

Previous research[2] has shown that water cooling is effective in achieving downsizing of the motor above 15 kW. However, the previous report focused only on the concentrated winding and did not mention motors with SC distributed windings, which have become popular recently.

Therefore, in this study, we have constructed an analytical model that allows for a side-by-side comparison of the motor winding and cooling systems of electric motorcycles. Using this model, we have organized the optimal combinations of winding and cooling systems for each vehicle output, and have confirmed the validity of the combinations used in commercially available EVs.

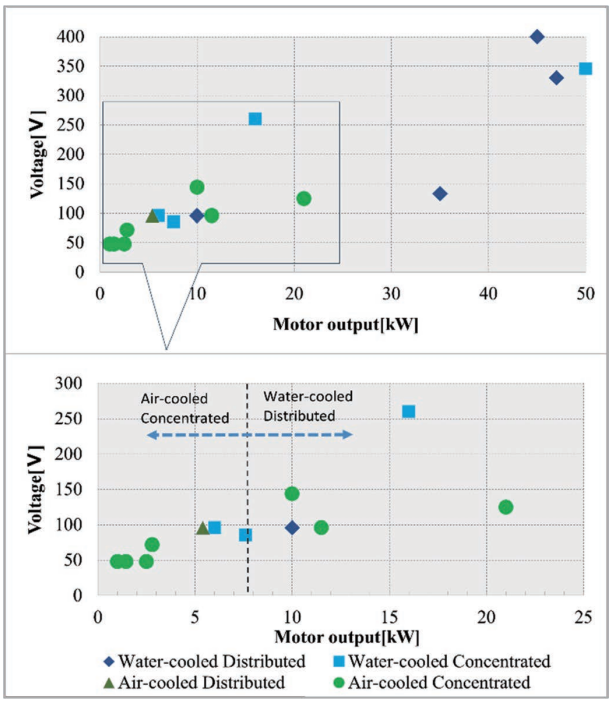

Fig. 1 Winding types and cooling methods

In order to verify the above, two types of motors were designed: one with a concentrated winding and the other with a distributed winding. A magnetic field analysis model was prepared for each motor.

By improving the winding fill factor, the thermal 1 from the coil to the stator can be reduced, which in turn reduces the temperature rise[3]. In the motor configuration designed in this article, we have employed a concentrated winding coil utilizing rectangular wire or a distributed winding with SC, which are believed to possess a high fill factor and superior heat dissipation capabilities.

In the thermal design of motors, the losses of each component vary depending on the operating point of the output, and the way in which the temperature of each component rises is also different[4]. Therefore, in order to correctly calculate the temperature rise of the motor, it is necessary to define the operating point of the motor for each vehicle output, calculate the losses in each part, and then perform a thermal analysis.

One method of thermal analysis for motors is to calculate

temperature rise with high accuracy by bidirectionally coupling magnetic field analysis with thermal and fluid analysis[5]. However, in this study, it is necessary to perform multiple case calculations for motors with different power and cooling methods, and the calculation time becomes enormous. One method to reduce the calculation time is the thermal equivalent circuit network method. In this method, the thermal resistance and thermal capacity on the main thermal path are modeled to estimate the temperature rise of the motor[6]. Although this method is less accurate than thermal fluid analysis, it is considered accurate enough for the relative comparisons required in this study. Therefore, in this study, we attempted to reduce the calculation time by constructing an equivalent thermal circuit model that includes the effects of the radiator and driving wind on motorcycles based on a CFD model[7] that has been confirmed to have sufficient accuracy within Yamaha.

2 MODEL FOR VERIFICATION

2-1. The Configuration of the Motor

In order to facilitate the verification process, we have designed a concentrated winding motor and an SC motor, each of which is intended to be installed in a motorcycle that is equivalent to a European A1-A2 license. The concentrated winding motor is a 12-slot, 8-pole Interior Permanent Magnet Synchronous Motor (IPMSM). The winding is composed of a rectangular wire. The stator core is divided at the teeth and each tooth is wound with an insulating bobbin. This structure increases the space factor, which increases the adhesion between the coils and the insulating bobbin and improves the heat dissipation capacity.

The SC motor has 48 slots and 8 poles and uses rectangular wires.

The stator outer diameters of the respective motors are equivalent. Heat is transferred to the case by shrinkage fitting the stator core to the aluminum case.

For water-cooled motors, cooling channels are provided in the aluminum case. In the case of air-cooled motors, fins are provided on the outer diameter of the aluminum case (Figure 2). The core length of the motor is adjusted to achieve the appropriate torque and output characteristics in accordance with the performance requirements of the vehicle. In this process, the cross-sectional shape of the motor remains unchanged, and the aluminum case, water cooling channels, fins and coils are extended accordingly (Figure 3).

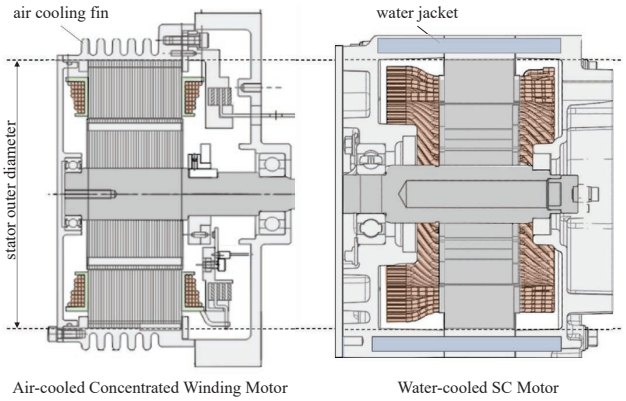

Fig. 2 Example of Drawings of Motors

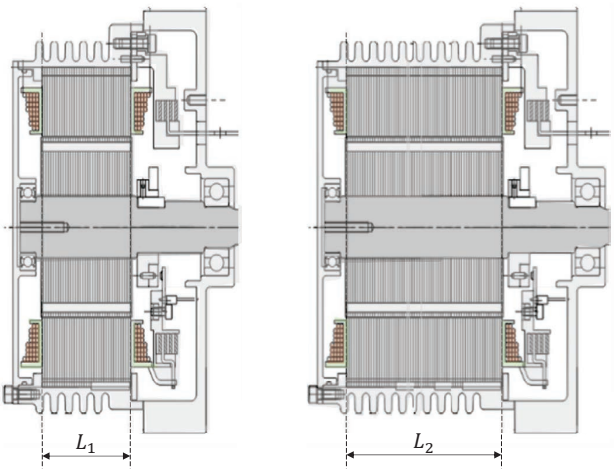

Core Length $L_1 < L_2$

Fig. 3 Example of Motors with Different Core Lengths

In order to facilitate discussion of motor size in the following sections, it is necessary to define motor volume. The calculation of motor volume is performed as a cylindrical shape. The diameter shall be the outer diameter of the aluminum housing. In this study, water-cooled and air-cooled motors will be treated, and the outer diameters of the water-cooled jacket and air-cooled

fins will be assumed to be equal. Consequently, the difference between water-cooled and air-cooled motors has no effect on the outer diameter of the motor. The cylinder length shall be equal to the height of the coil. Since the height of the coil end differs between concentrated winding and SC, the volume differs even with the same core length. Therefore, the volume of the motor to be compared is as shown in Figure 4.

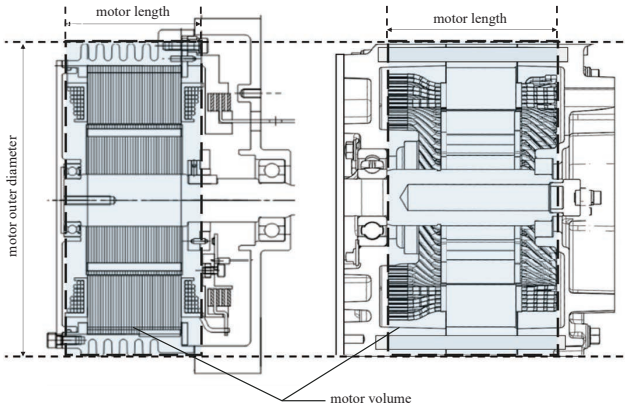

Fig. 4 Definition of motor volume

In an actual motor, there is a shaft and housings at both ends, but these are considered equal regardless of the motor type and are not considered in the volume comparison.

However, the specific heat and thermal resistance of the shaft and housing are considered in the thermal analysis described below.

2-2. Cooling Systems

An overview of the cooling system of the water-cooled electric motorcycle assumed in this study is shown in Figure 5. In the case of a water-cooled motor, the motor and inverter have cooling jackets, and the heat is exchanged with the outside air through a radiator. The motor cooling jacket is located at the periphery of the aluminum housing. The outside air is assumed to flow equally around the radiator and the motor housing at a flow rate calculated from the vehicle speed and the vehicle speed utilization ratio. The weight and volume of the reservoir tank and electric water pump are also considered components of the cooling system.

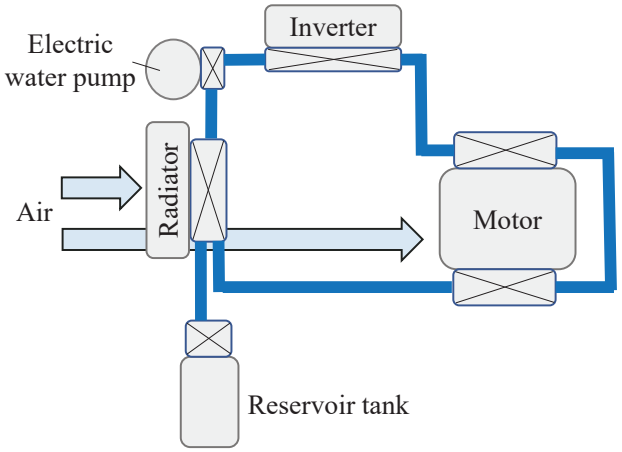

Fig. 5 Cooling System of Water-cooled Motorcycle

In the case of air cooling, cooling fins instead of water jackets must be provided for both the motor and the inverter. Water cooling systems such as radiators are not installed in the air-cooled vehicle. Cooling air equivalent to that of the water-cooled case hits the cooling fins of the motor housing and exchanges heat.

2-3. Thermal Circuit Model of a Motor

A thermal circuit model of a motor is described. The motor losses considered are copper loss in the coil, iron loss in the core, joule loss in the magnet, and friction loss in the bearing and oil seal. The losses generated in each part are dissipated to the outside air or cooling water according to the thermal circuit model shown in Figure 6.

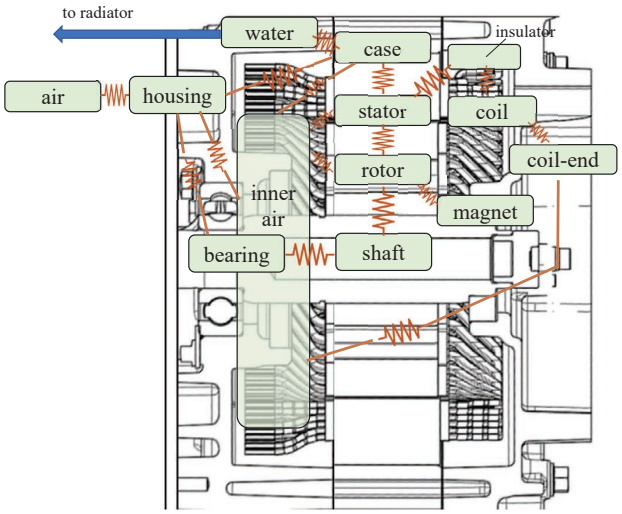

Fig. 6 Thermal Circuit Model of a Motor

3 ANALYSIS MODEL

3-1. Vehicle Model

In order to identify the optimal combination of winding and cooling system for each output, it is necessary to define the performance of the vehicle for each output. In this study, vehicles with a maximum output of 5 to 35 kW were considered, which corresponds to the European A1 to A2 license range for internal combustion engine (ICE) vehicles. Previous studies have demonstrated a correlation between rear wheel output, maximum driving force, and speed in a typical internal combustion engine (ICE) motorcycle[2]. Consequently, the aforementioned correlation was employed once more to define the required driving force and maximum speed for each vehicle with varying power outputs. Figure 7 illustrates the correlation. For example, a vehicle with a maximum output of 8 kW requires a driving force of 1029 N and a maximum speed of 102 km/h.

In the thermal design of motors, it is crucial to consider not only the maximum output but also the continuous rated output. However, there is no universally accepted definition of continuous rated output for. Therefore, in this study, we defined the thermal performance to be met as the ability to continuously deliver the maximum power of the vehicle for 15 minutes at 60% of the maximum speed of the vehicle, which is assumed to be used frequently.

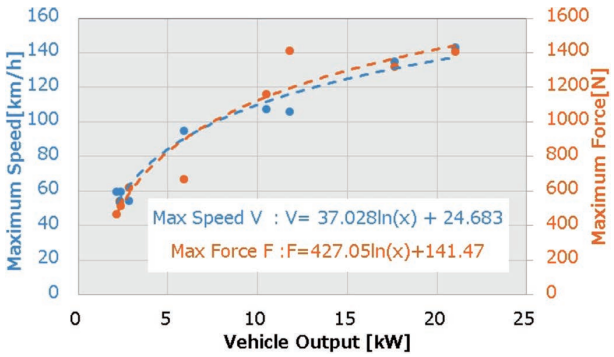

Fig. 7 Correlation between Vehicle Power and Maximum Driving Force and Speed in ICE Motorcycle

It is assumed that the size of the battery varies with vehicle output. In particular, the model assumes that the DC voltage of a vehicle with a maximum output of 10 kW is 100 V, and that it increases or decreases linearly with vehicle output.

3-2. Cooling System Model

The cooling system depicted in Figure 5 as implemented in each vehicle output in the following manner. The radiator was designed to have a variable size. The radiator's heat dissipation capacity was modeled to be contingent upon the wind speed and radiator size. The radiator's speed utilization factor varies with the vehicle configuration; however, in this study, it was assumed to be constant at 0.2. Consequently, the wind speed utilized by the radiator is contingent upon the vehicle speed at rated output and the vehicle speed utilization ratio. The outside air temperature was fixed at 25°C. Figure 8 illustrates the relationship between radiator size, vehicle speed, and heat dissipation for the radiator model created.

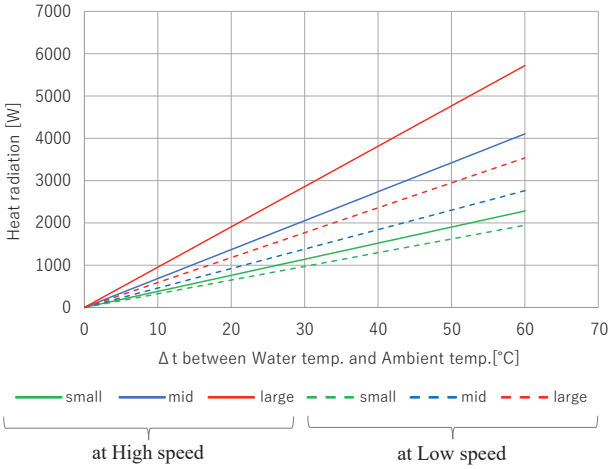

Fig. 8 Relationship between Radiator Size, Vehicle Speed, and Heat Dissipation for the Radiator Model

The following section will discuss the other components considered in the cooling system. It was assumed that the electric water pump would be a commercially available 12 W product, regardless of vehicle power, as was done in previous studies. In the vehicle under study, the flow rate was assumed to be 5 l/min, as the pump has sufficient capacity. The volume of the pump is 251 cc, and its weight is 0.4 kg. The cooling hose utilized for the vehicle is assumed to be Φ22, 400 mm in diameter. The

total volume of cooling water will vary according to the size of the motor and the radiator. For water-cooled vehicles, the volume and weight of these cooling systems must be considered in addition.

3-3. Magnetic Field Analysis Model

Each loss of the motor at the rated output set by the vehicle model was calculated using a two-dimensional magnetic field analysis model. The calculated losses included AC and DC copper losses, Joule losses of the magnets, and iron loss. Actual measured values were used for the mechanical losses of bearings and oil seals. In order to accurately analyze the losses generated in the motor, it is necessary to consider that the actual motor current includes harmonic components due to the pulse width modulation (PWM) control of the inverter. However, magnetic field analysis that reproduces PWM control requires a significant amount of time for computation. Therefore, in this study, we compared the analysis results using the ideal sine wave current with those considering PWM harmonics, and coefficients were calculated for the effect on loss. Subsequently, the aforementioned coefficients were applied to the results of the ideal sine wave analysis in order to achieve a closer approximation of the actual motor losses. For simplicity, the loss distribution of each component was not considered, and each loss was assumed to occur uniformly in each component of the thermal analysis model. In the 2D magnetic field analysis, the copper loss at the coil end cannot be calculated. Consequently, the copper loss at the coil end was calculated based on the current value and input to the coil end of the thermal circuit model.

The accuracy of the loss calculations was validated by comparing the magnetic field analysis model with the measurement results of the actual equipment. As an example, Table 1 Comparison of Motor Loss Analysis and Measurement depicts the analysis results of an SC motor under specific operational conditions and the measured efficiency of the actual motor. The discrepancy between the calculated and measured losses of the actual motor was approximately 5%, thereby confirming that this analytical model is sufficiently accurate.

Table 1 Comparison of Motor Loss Analysis and Measurement

Analyzed Losses [W]			
Copper Loss	269.8		
Stator Loss	280.2		
Rotor Loss	32.6		
Magnet Loss	77.2		
Total Loss	***659.9***	Measured Motor Loss	***631.7***

3-4. Method for the Design of Motors according to Vehicle Output

In this study, it is assumed that the motor output characteristics are adjusted by varying the core length without changing the motor cross-sectional shape (i.e., magnetic circuit). Therefore, it is necessary to design an appropriate core length for each vehicle output. The procedure is described below.

(1) As previously stated in the section on the vehicle models, the DC voltage, required driving force, and maximum vehicle speed are determined according to the vehicle's maximum output.

(2) The maximum rotational speed of the motor is considered to be 12,000 rpm or less. This analysis considers the rotational speed range of bearings and oil seals typically employed in motors, excluding those with exceedingly high rotational speeds.

(3) Since the motor cross-section does not change from the initial design, the minimum motor size (core length) required to meet the driving force requirements of the vehicle is determined. The N-T characteristics and efficiency of this motor are determined by magnetic field analysis.

(4) The efficiency map of the motor is obtained through magnetic field analysis. The speed at which the motor can operate at high efficiency is identified, and this point is defined as the rated point. In other words, this speed represents 60% of the vehicle's maximum speed. This enables us to posit the vehicle's reduction ratio. In the event that the requisite maximum rear-wheel drive force

cannot be attained at the assumed reduction ratio, it is necessary to adjust the reduction ratio within the range where the motor efficiency at the rated point remains relatively unchanged. Should this prove insufficient to meet the requisite driving force for the vehicle, it will be necessary to adjust the dimensions of the motor.

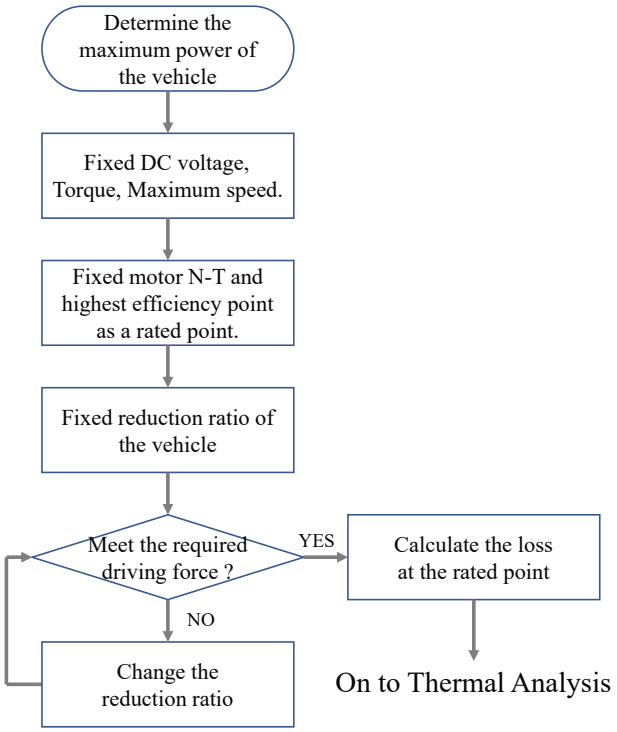

Fig. 9 Motor Design Procedure

A multitude of combinations of motor size and reduction ratio can be found that satisfy the requirements of the vehicle. Among these combinations, the configuration that satisfies the thermal performance requirements at the rated point and minimizes the total volume of the cooling system and motor is sought through thermal analysis. The methodology for identifying the optimal minimum size will be described in a subsequent section.

3-5. Thermal Analysis Model

The magnetic field analysis model enables the determination of the motor size and losses during rated operation. Consequently, the thermal resistance between the parts in the motor can be calculated based on the motor's body size. Furthermore, the heat capacity of each component and the volume of cooling water can be determined.

Thermal analysis was conducted by reproducing the thermal circuit depicted in Figure 5 and Figure 6 in JMAG, a magnetic field analysis software. To reduce the time required for calculations, the analysis was conducted by combining the FEM analysis in JMAG and the thermal circuit model. In the FEM analysis, the heat transfer in the electromagnetic part of the motor that generates the loss was evaluated. The thermal circuit model reproduced the heat dissipation to air and other fluids, as well as the thermal resistance of the contact area of the parts receiving the heat dissipation. The thermal circuit model also reproduced the shaft, motor case, cooling jacket, and vehicle radiator, excluding the electromagnetic parts.

The thermal resistance of each component was incorporated into the circuit model through the application of the equivalent thermal conductivity equation (Figure 10, e.q.(1), e,q.(2)).

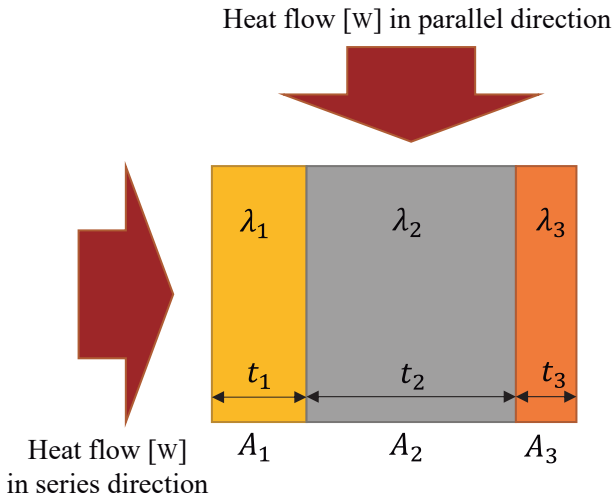

Fig. 10 Heat flow in series and parallel

$$\lambda_{eq\_S} = \frac{t}{\sum \frac{t_i}{\lambda_i}} \quad (1)$$

$$\lambda_{eq\_P} = \frac{\sum (A_i \cdot \lambda_i)}{A} \quad (2)$$

λ_{eq_S} : Equivalent Thermal Conductivity in Series
λ_{eq_P} : Equivalent Thermal Conductivity in Parallel
t : Total Thickness
t_i : Thickness of each Component

λ_i : Thermal Conductivity of each Component
A : Area in the Direction of Heat Flow
A_i : Area of each Component in the Direction of Heat Flow

The contact area between components is typically quantified by an index known as contact thermal resistance. In this model, the calculation was based on Tachibana's equation[8], a widely utilized expression for contact thermal conductance, with adjustments made based on actual measurements.

$$K = \left(\frac{1.7 \times 10^5}{\frac{\delta_1 + \delta_0}{\lambda_1} + \frac{\delta_2 + \delta_0}{\lambda_2}} \cdot \frac{0.6P}{H} + \frac{10^6 \lambda_f}{\delta_1 + \delta_2} \right) \cdot C \quad (3)$$

K : Contact Thermal Conductance [$W/(m^2 \cdot K)$]
$\delta_{1,2}$: Maximum Height of each Part Surface Roughness [μm]
δ_0 : Contact Equivalent Length [μm]
λ_f : Fluid Thermal Conductivity [$W/(m \cdot K)$]
P : Contact Pressure [MPa]
H : Vickers Hardness of the Softer Side[kg/mm^2]
C : Correction Factor

The validity of the thermal analysis model was verified by comparing it with the actual motor. The thermal analysis model was partially calculated using a thermal circuit, which resulted in the analyzed temperatures being volume-averaged temperatures. Conversely, since the surface temperature of each component was measured in the experiment, it cannot be directly compared with the results of this analysis. Consequently, a computational fluid dynamics (CFD) thermal analysis model[7] was employed to assess the thermal circuit model developed in this study. This validated the efficacy of the thermal circuit model. Initially, the outcomes of the CFD full model analysis and the actual machine were compared. The evaluation conditions are the results of running at a constant output for one hour at an ambient temperature of 25 degrees C and natural air cooling. The analysis is also based on the same conditions.

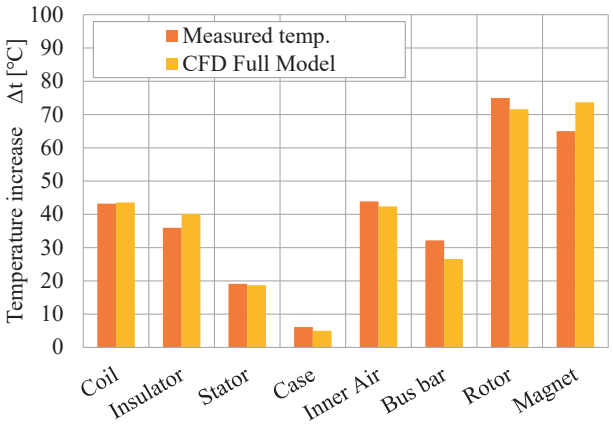

Fig. 11 Comparison of CFD Analysis Temperatures and Experimental Results

Figure 11 shows that the CFD model is sufficiently accurate, with an error within 10% of the experimental results. Therefore, the volume-averaged temperatures of each component were obtained from the CFD model. The accuracy of the thermal circuit model was confirmed by comparing the CFD results with the analysis results of the thermal circuit model used in this study. The results of the comparison are shown in Figure 12. This result demonstrates that the thermal circuit model is sufficiently accurate for relative comparisons of cooling performance between different motors. The analysis using the thermal circuit network model is a transient analysis with 10 seconds per step, and the results shown are those at the point in time when the same amount of time has elapsed as in the actual machine evaluation. The residual value of less than 10^{-8} has been set as the convergence criteria for each step.

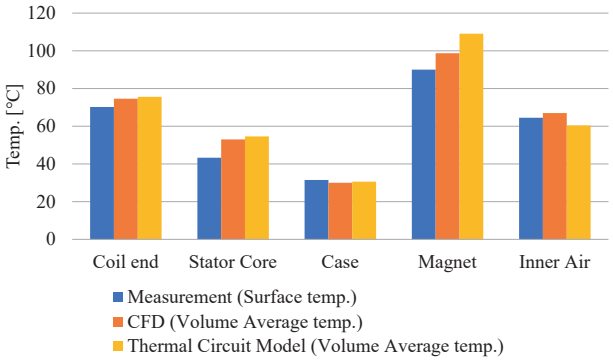

Fig. 12 Comparison of CFD Analysis Temperatures and Thermal Circuit Model

The subsequent section of this discussion will examine the comparative characteristics of motors with distinct winding configurations and varying core lengths. It is important to note that concentrated winding and SC have disparate coil shapes, which consequently affects the contact area between the coil and the core. The larger the contact area, the lower the thermal resistance. In general, SC exhibits a larger contact area between the coil and core due to the ease of increasing the number of slots, which results in superior heat dissipation (Figure 13). Conversely, concentrated winding has smaller coil ends. Consequently, if the core length is identical to that of the SC, it can be reduced in size. In the motor under consideration, the contact area between the coil and core is 2.3 times larger and the coil end size is 1.2 times larger than that of the concentrated winding motor. This value is considered in the present study.

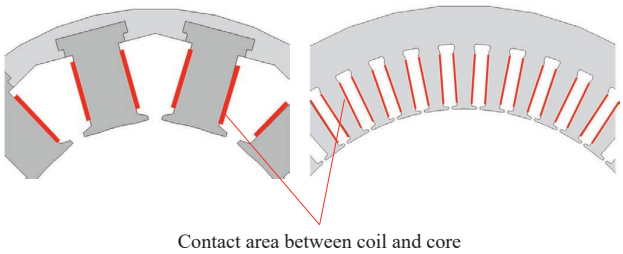

Fig. 13 Difference in contact area between concentrated winding and SC

For motors with different core lengths, the thermal resistance of each part changes as described above. A motor with a larger core length is capable of more heat dissipation and has a larger heat capacity, which changes the temperature rise during vehicle operation. Conversely, the larger motor volume increases the phase resistance of the coil, which may result in increased copper loss, and the larger core volume may increase the iron loss.

The following definitions pertain to other conditions.
For the sake of simplicity, the change in volume of the gear section due to the reduction ratio is not considered. Furthermore, the size and mass of the inverter are not considered, as the focus is on the motor. The water temperature shall be limited to 60℃. In the case of water-cooled motors, the inverter is generally water-cooled as well. Therefore, the upper water temperature limit is set in consideration of inverter cooling. The upper temperature limit for coils and magnets varies depending on the selection of materials, but in this case, the upper temperature limit for both is 160°C. If the temperature of each of the components does not exceed the upper limit, the motor is deemed to have sufficient thermal rating capacity. However, if the temperature exceeds the upper limit, the motor should be enlarged to improve the heat dissipation capacity, or the radiator size should be increased to identify the smallest size that can achieve the rated output.

3-6. Optimization Procedure for each Motor Output

The following procedure outlines the specific methodology for comparing motor and cooling system sizes for each output. As previously stated, the design of the motor should be based on the output to be considered. The loss of the motor in rated operation is determined by magnetic field analysis. Given that the size of the motor is fixed, the thermal resistance and heat capacity of each component can be obtained. The thermal analysis model determines the heat dissipation capacity of the radiator based on the vehicle speed at rated operation and the radiator size. The considerations thus determine the conditions for the thermal circuit model.

(1) The motor temperature should be assessed using the thermal circuit model that has been determined.

(2) If the temperature exceeds the upper limit, the radiator size should be increased so as to improve the capacity for heat dissipation.

(3) The thermal analysis should be repeated with the new model.

(4) If a model is identified within the temperature limit, the volume and weight of the motor and cooling system should be calculated.

(5) The motor core length should then be increased. It is necessary to ascertain whether a combination can be

achieved with a smaller radiator size due to the increased heat dissipation capacity of the motor.

(6) The procedure should be repeated (1) to (5) in order to extract the smallest combination of motor and cooling system that satisfies the thermal rating.

In the case of air-cooling, there is no radiator, thus the sole means of increasing the heat dissipation capacity is to increase the motor size.

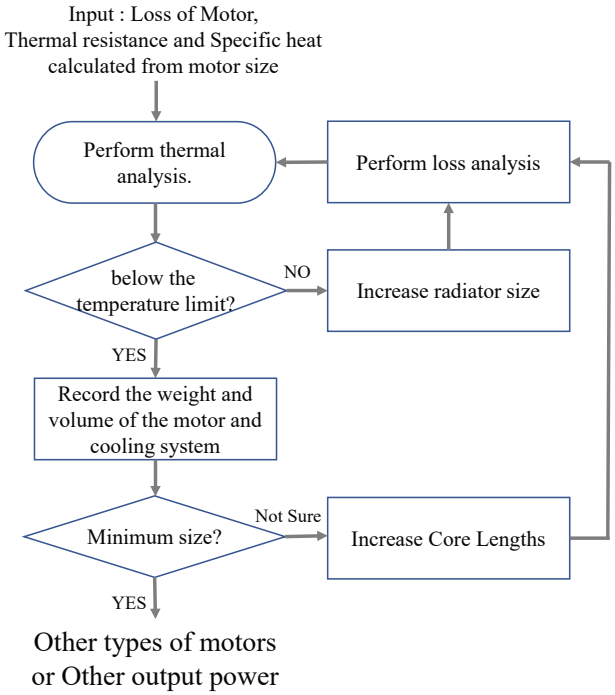

Fig. 14 Optimization Procedure

4 ANALYSIS RESULTS

4-1. Results for Vehicles with a Maximum output of 11 kW

As an example, the results of the study are presented for a vehicle with a maximum output of 11 kW when an SC water-cooled motor is applied. The vehicle model is defined in accordance with the specifications outlined in Table 2.

Table 2 Specifications of Vehicle with Maximum output of 11 kW

Max. Power [kW]	11
Max.Speed [km/h]	113.5
DC voltage [V]	110
Max. Force [N]	1165

The minimum core length required to achieve the desired vehicle performance was 35 mm. A thermal analysis was conducted on this motor in conjunction with a radiator of the smallest size. The results are presented with the core size held constant and the radiator size increased. The radiator size is expressed as a percentage of the radiator size utilized in the ICE 125cc vehicle.

Figure 15 presents the results of the analysis. When the core length is 35 mm, there is a margin for coil and magnet temperatures for all radiator sizes. The water temperature falls below 60°C when the radiator size is 63%. Therefore, when the motor core length is 35 mm, 63% radiator size is required.

The subsequent step is to ascertain whether the overall volume and weight can be reduced by increasing the core length and decreasing the radiator size. This same study is conducted for a motor with a core length of 40 mm as for 35 mm. The results indicate that at 40 mm, a radiator size of 42% is sufficient because the heat dissipation capacity of the motor has been improved.

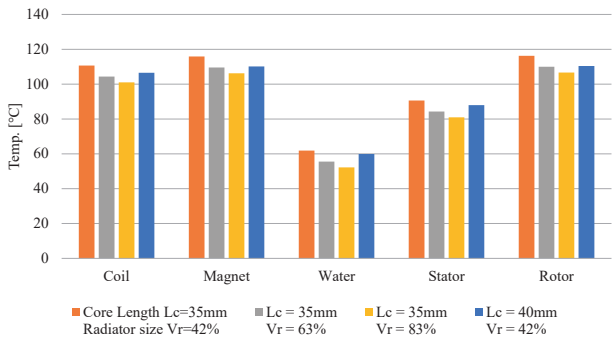

Fig. 15 Results of Thermal Analysis on a 11 kW Vehicle

In the context of a typical motorcycle, it is not appropriate to consider radiators smaller than 42%. Consequently, the smallest possible combinations are either a 35 mm

core length with 63% radiator or a 40 mm core length with 42% radiator. The results of this comparison are presented in Figure 16.

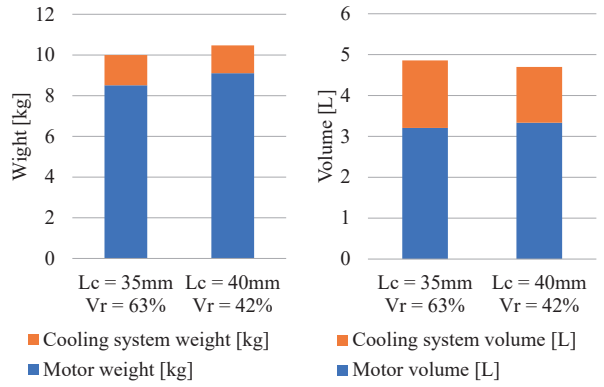

Fig. 16 Comparison of Motors with different Core Lengths

The results indicate that the lightest weight is observed at a core length of 35 mm, while the smallest volume is observed at a core length of 40 mm. Similar studies were conducted with different winding types, cooling methods, and power outputs.

4-2. Summary of Study Results for each Output

The total weight and volume of the four combinations were compared: concentrated winding, SC, air-cooled, and water-cooled. The volume and weight of the water-cooled SC were used as a reference for relative comparisons of the other combinations. The volume comparison results are shown in Figure 17.

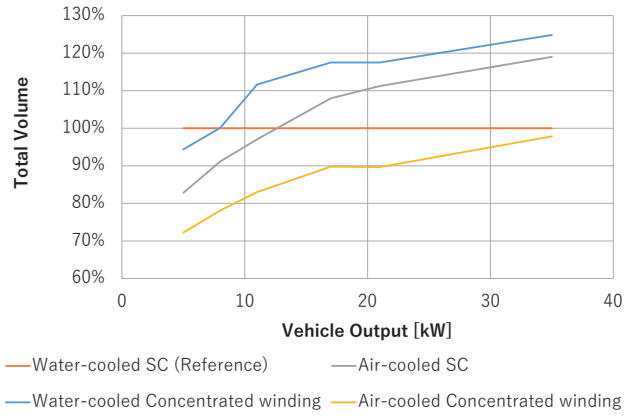

Fig. 17 Volume Comparison Results

It was found that air-cooled concentrated winding motors have the smallest volume in the range of 35 kW or less. For motors of 15 kW or more, the volume of water-cooled SCs is 110% or less of that of air-cooled concentrated windings, so they can be considered roughly equivalent.

When comparing water-cooled SC motors with water-cooled concentrated motors, it can be seen that the SC is superior in terms of miniaturization in almost all areas except 5kW. In this study, motor cooling is achieved by a cooling jacket on the outer case of the motor. On the other hand, concentrated winding motors have higher thermal resistance than SC due to the difference in contact area between the coil and the core. Therefore, SC can cool the motor more efficiently. Although concentrated winding reduces copper and stator losses compared to SC, it cannot achieve the miniaturization effect of water-cooled SC motors.

The number of slots in an SC motor can be increased more easily. This reduces the eddy current loss generated in the magnets inside the rotor compared to a concentrated winding motor. Since the rotor has no cooling jacket, the temperature rises more easily as the loss increases. Figure 18 shows the temperature results for a 5 kW SC water-cooled motor and a concentrated winding water-cooled motor. The core length of both motors is 30 mm and the size of the cooler is the same. The water temperature is almost the same (55-60°C), but the temperature of each part is higher in the concentrated winding motor. This indicates that the heat resistance of the concentrated winding motor is higher. *The thermal resistance between the housing and the cooling water is very small for both the concentrated winding motor and the SC motor, so the temperature of the housing is mainly affected by the cooling water temperature. In this result, the water temperature was slightly lower in the concentrated winding motor, so only the case temperature was reversed.

Air-cooled SC motors also failed to demonstrate superiority over other methods. This is probably because while SCs have excellent heat dissipation characteristics due to their low thermal resistance from the coil to the housing, air cooling can only achieve limited heat

exchange from the housing to the air, so it cannot demonstrate its heat dissipation performance.

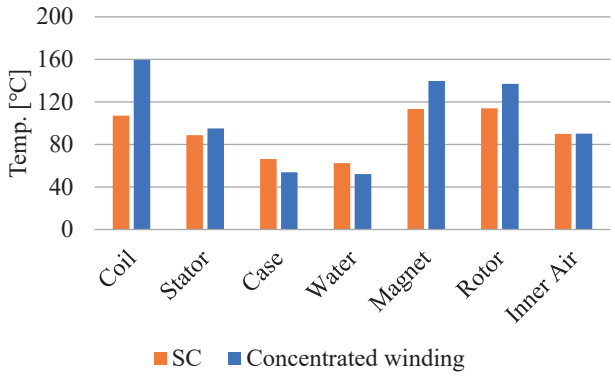

Fig. 18 Temperature Comparison between Concentrated Winding and SC

The next step is to compare the weights. The results are shown in Figure 19.

In terms of weight, the 5 kW rated unit is slightly superior to the water-cooled concentrated winding motor. However, in all other cases, the water-cooled SC motor is the best. For 10 kW and below, air cooling is superior in volume, but water cooling is superior in weight. This is due to the weight density of the motor. The construction of motors comprises electromagnetic steel and copper, which have a high weight density. In contrast, water-cooled systems such as radiators and pumps have a low weight density. In air-cooled motors, core length is increased to enhance heat dissipation, which has a significant impact on weight. In water-cooled motors, the size of the radiator can be expanded to improve cooling capacity, thereby reducing weight.

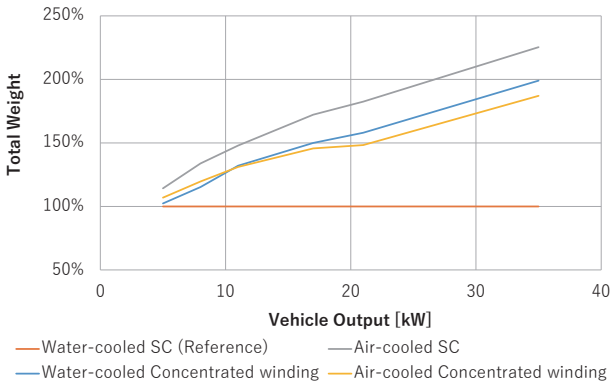

Fig. 19 Weights Comparison Results

Finally, the relationship between heat dissipation capacity and volume or weight is shown in Figure 20 and Figure 21. Figure 20 shows the results of a study on a water-cooled SC motor with an output of 35 kW. It compares the effects of increasing the core length and radiator size to enhance heat dissipation capacity. In both cases, the temperature decreases with an increase in volume. The reduction in temperature per volume was validated using coil temperature as an indicator.

As a result, when comparing the effects of increasing the length of the motor core and increasing the size of the radiator, it was found that the effect of reducing the coil temperature per unit volume was better when the core length was increased. Figure 21 shows the effect of temperature reduction in relation to the change in weight. In terms of weight, the effect of increasing the size of the radiator is equivalent to increasing the size of the motor. When cooling the coil temperature, it can be seen that increasing the contact area with the housing, which is the main heat sink for the coil, is more effective in reducing the temperature than increasing the size of the radiator. This trend is the same for the rotor (Figure 22, 23).

On the other hand, Figures 24 and 25 show the relationship with water temperature. Figure 25 shows that if you want to reduce the water temperature, it is much easier to increase the radiator size than to increase the core length.

Therefore, to reduce the temperature inside the motor, it is more effective to increase the size of the motor itself, increase the heat exchange area, and reduce the thermal resistance, but you must be careful not to increase the weight. Increasing the size of the radiator is useful for reducing the water temperature.

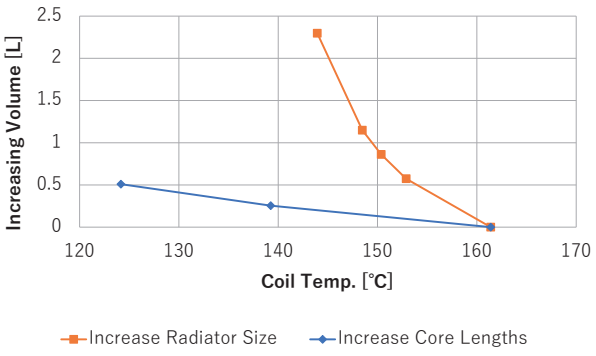

Fig. 20 Relationship between Coil Temperature and Volume

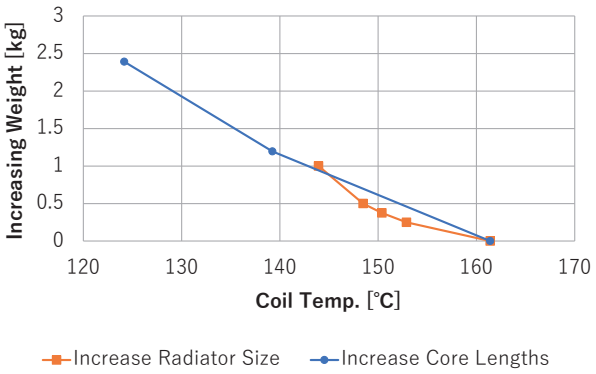

Fig. 21 Relationship between Coil Temperature and Weight

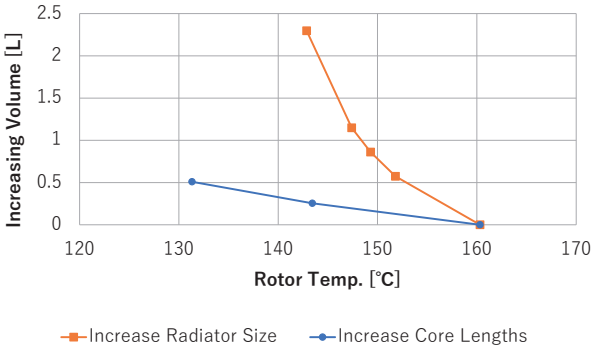

Fig. 22 Relationship between Rotor Temperature and Volume

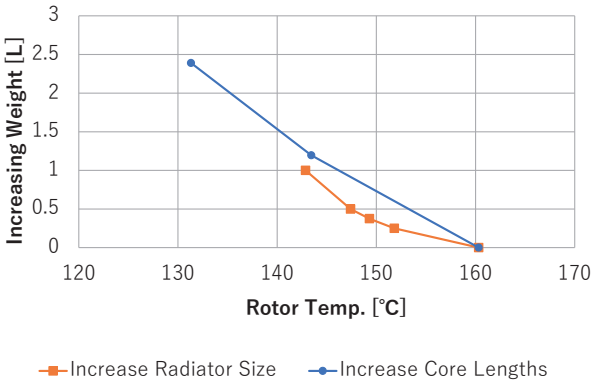

Fig. 23 Relationship between Rotor Temperature and Weight

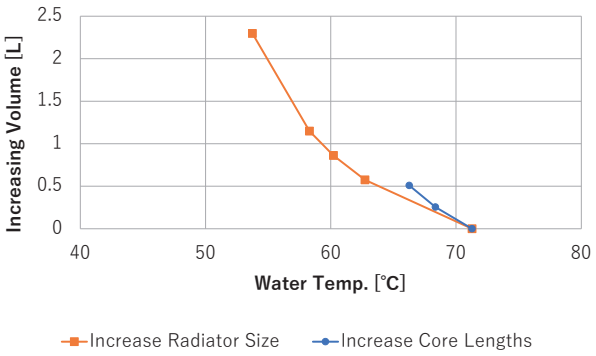

Fig. 24 Relationship between Water Temperature and Volume

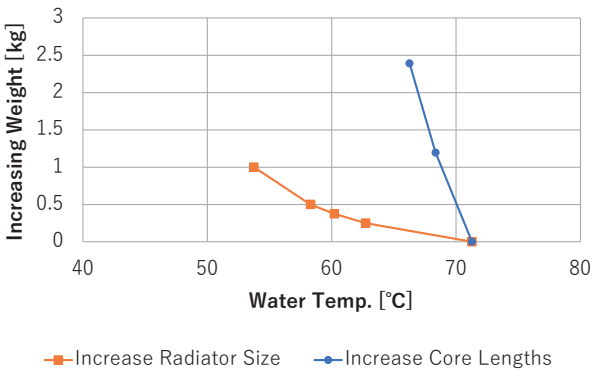

Fig. 25 Relationship between Water Temperature and Weight

5 SUMMARY/CONCLUSIONS

In order to compare the combination of winding methods and cooling systems in the output range of European A2 licenses and below, we constructed an analysis model using magnetic field analysis and thermal circuit networks.

Using this model, we examined the smallest power unit configuration, including the cooling system, for each vehicle output.

For the motor we designed this time, we found that the air-cooled concentrated winding motor had the smallest volume when the vehicle output was 35 kW or less. On the other hand, the water-cooled SC motor was the lightest in all power ranges. In the 15 kW and above range, it was found that the water-cooled SC motor was about the same size as the air-cooled concentrated winding motor, even when the water-cooling system was included.

Therefore, it was suggested that the air-cooled concentrated winding motor was superior in the range of 15 kW and below, and the water-cooled SC motor was superior in the range of 15kW and above.
These results are broadly consistent with the trends seen in commercially available EVs.

In the context of actual vehicle development, it is believed that the optimal combination may vary depending on the vehicle's specific performance requirements, motor design, and cost considerations. However, the use of this model has facilitated a more straightforward comparison of design proposals.

In the field of motorcycle design, it is important to select the most suitable motor and cooling system for the intended use. The findings of this research will prove an effective tool for making such decisions and may be applied in future vehicle development.

REFERENCES

[1] Yaohui Gai, Mohammad Kimiabeigi, Yew Chuan Chong, James D. Widmer et al.,"Cooling of Automotive Traction Motors: Schemes, Examples, and Computation Methods" IEEE Transactions on Industrial Electronics (Volume: 66, Issue: 3, March 2019), doi:10.1109 /TIE.2018.2835397
[2] Tsukasa Shimizu, Jin Itou, Hideki Shirazawa, Yasuyuki Muramatsu, "Study on appropriate cooling systems according to output of motor for small EV's" SAE Technical Paper 2017-32-0079, 2017, doi: 10.4271/2017-32-0079
[3] Norihisa Iwasaki, Hideki Kitamura, Masashi Kitamura, Junnosuke Nakatsugawa et al., "The Effect of Structure and Material Properties of Permanent Magnet Synchronous Motors on Temperature rise" IEEJ Rotating Machinery Research Committee (In japanese) Vol. RM-10 No. 134-152 Page. 61-66 (2010.10.20)
[4] Sasaki Kensuke, Akatsu Kan, "Effect of Cooling Methods on Continuous Output Capability of a Permanent Magnet Synchronous Motor" IEEE Conference Proceedings Vol. 2023 No. IEMDC Page. 1-5 (2023), doi:10.1109/IEMDC 55163.2023.10238898
[5] Tikadar Amitav, Kumar Nitish, Joshi Yogendra, Kumar Satish, "Coupled Electro-Thermal Analysis of Permanent Magnet Synchronous Motor for Electric Vehicle" IEEE Conference Proceedings Vol. 2020 No. ITherm Page. 249-256 (2020), doi: 10.1109/ITherm 45881.2020.9190562
[6] Norihisa Iwasaki, Hideki Kitamura, Masashi Kitamura, Junnosuke Nakatsugawa et al., "Miniaturization Design and Performance Evaluation of Prototype Permanent Magnet Synchronous Motor Optimally Designed with Thermo-Magnetic Field Coupling Analysis" IEEJ Rotating Machinery Research Committee (In Japanese) Vol. RM-10 No. 56-69 Page. 57-62 (2010.05.28)
[7] Takuya Yamauchi, Satomi Ishikawa, Mika Inoue, Hideki Oki, "Modeling methods that contribute to improvements in accuracy of CFD analysis on electric motor" Yamaha Motor Technical Review No. 57, Dec. 2022.
[8] Fujio Tachibana, "A Study on the Thermal Resistance of Contact Surfaces" Transactions of the JSME (in Japanese), Vol. 55, No. 397, pp. 102–107, 1952, doi: 10.1299/jsmemag. 55.397_102

■著者

大滝 亮太
Ryota Otaki
パワートレインユニット
プロダクト開発統括部
電動 PT 開発部

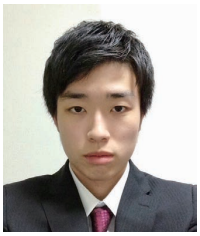

土屋 照之
Teruyuki Tsuchiya
技術・研究本部
技術開発統括部
先進プロダクト開発部

酒井 悠
Yu Sakai
パワートレインユニット
プロダクト開発統括部
電動 PT 開発部

山内 拓也
Takuya Yamauchi
技術・研究本部
技術開発統括部
制御システム開発部

清水 司
Tsukasa Shimizu
パワートレインユニット
プロダクト開発統括部
電動 PT 開発部